Original research or treatment paper

# Analysis and conservation of modern modeling materials found in Auguste Rodin's sculptures

**Juliette Langlois[1], Guylaine Mary[2], Hélène Bluzat[2], Agnès Cascio[2], Nathalie Balcar[1], Yannick Vandenberghe[1], Marine Cotte[3,4]**

[1]Centre de Recherche et de Restauration des Musées de France, Paris, France, [2]Freelance Conservator, Paris, France, [3]European Synchrotron Radiation Facility, Grenoble, France, [4]Laboratoire d'archéologie moléculaire et structurale (LAMS), CNRS UMR Sorbonne Universités, UPMC Univ. Paris, France

Prior to the exhibition *Portrait-making, Rodin and his models* (2009), the Rodin museum wanted to restore two busts of Hanako and Clemenceau. Interestingly, these two sculptures contain pieces of modern modeling materials (MMMs) invented at the end of the nineteenth century as an alternative to clay or waxes. The poor state of conservation of the two portraits made any handling and exhibition impossible. Accordingly, the purpose of this article is twofold: to contribute to technical art history and conservation. Elemental and chemical analyses were done on samples from 12 sculptures (SEM–EDX, FTIR, GC–MS, GC–FID, XRD, synchrotron-based μXRF, μXANES, and μFTIR) aimed at identifying the composition of MMMs used by Rodin on plaster sculptures and establishing hypotheses about the origins of their degradation. This thorough study of their composition and degradation was necessary to implement an appropriate restoration plan. The development of conservation protocols adapted to such materials is rarely documented. Different tests were performed on mock-ups (pH, solubility, adhesion, consolidation, and cleaning). In particular, a protocol based on laser cleaning was developed and successfully applied to remove superficial dust and crusts so that the sculptures regained their original aspect.

**Keywords:** Rodin, Sculpture, Modern modeling material, Plastiline, Conservation, Adhesives, Laser cleaning, Carboxylate

## Introduction

### Context

This research started thanks to the wish of the Rodin museum to restore two plaster busts. These two busts, *Hanako* (S.02242; probably between 1908–1912; Fig. 1) and *Clemenceau* (S.01982; 1911–1913; Fig. 2), needed to be restored prior to being presented in the exhibition *La fabrique du portrait, Rodin face à ses modèles* (*Portrait-making, Rodin and his models*, Rodin Museum, 10 April–23 August 2009). Their poor state of conservation with active deterioration strongly affected handling. These models were a way for Rodin to practice repeatedly until achieving the optimum form. As such, they offer great insight into the creative process of the sculptor and the techniques he developed. These two busts contain some modern modeling materials (MMMs), which, in French, would be named *pâte à modeler*. A regular English denomination for such materials is *modeling clay*; however, it gives the wrong impression that the material systematically contains clay. As detailed below, these non-drying materials were invented during the nineteenth century, as an alternative to clay or beeswax. They can be present in various compositions (including clay or not) and names, which evolve with time and geographical origin, without a systematic correspondence to materials. To avoid confusion, we will use the generic name MMMs to refer to the full class of such synthetic materials, and specific terms such as Plastiline® only for commercial materials of controlled origin.

The purpose of this article is to present analytical studies of the compositions of MMMs used by Rodin on sculptures, to establish hypotheses about the origins of their degradation, and to present the protocols of conservation. In particular, it was important to investigate the correlations between the composition of the MMMs, their color (dark brown, brown ocher, gray, and ivory-colored), their use (bulk modeling material or localized modeling additions), and their diverse alterations.

Correspondence to: Juliette Langlois, Centre de Recherche et de Restauration des Musées de France, Palais du Louvre – Porte des Lions 14, quai François Mitterrand, 75001 Paris, France.
Email: juliette.langlois@culture.gouv.fr

© The International Institute for Conservation of Historic and Artistic Works 2016
Received 19 December 2015; revised paper accepted 04 November 2015
DOI 10.1080/00393630.2015.1131029

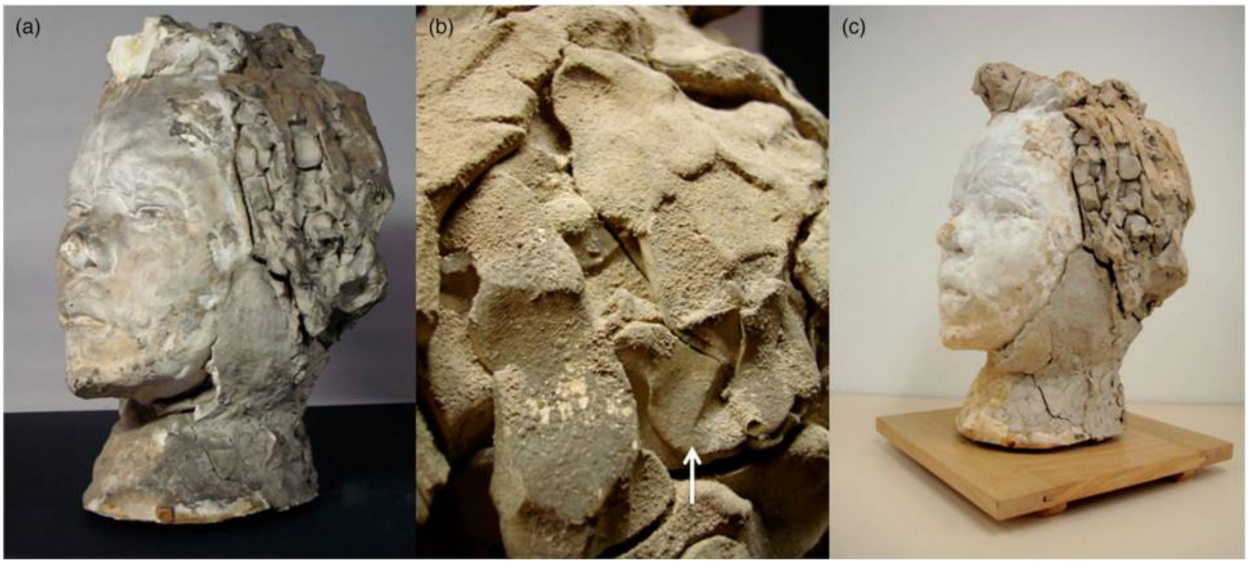


**Figure 1** ***Hanako*** **(S.02242, Musée Rodin, height: 53.5 cm, length: 41.6 cm, width: 37.9 cm). (A) Before conservation; (B) detail from** ***Hanako*** **sculpture showing finger print (highlighted with an arrow) and alterations of the MMM in the form of hard and rough black crust; (C) after conservation. Photo credits: H. Bluzat, A. Cascio, and G. Mary.**

## *Presence, use, and condition of MMMs in Rodin's works*

In 1906, Rodin, fascinated by the expression of the Japanese dancer and actor, Hanako, asked her to pose for him. He composed many drawings and models. The head of *Hanako* (Fig. 1) is one of these last models. The composition of the head is heterogeneous: the front consists of a plaster mask molded on the actress's face while the back of the head is loosely fashioned with pieces of plaster held together by the application of fresh plaster. The hair and a part of the neck are formed from an ivory-colored MMM applied after a preliminary reworking of the plaster with tools. In the reworked areas, the surface is therefore more irregular, thus facilitating the MMM's adherence.

This MMM was applied in heavy, large pieces. As a first step, it seems that Rodin outlined the areas where he wanted to add more volume by placing thinly rolled strips of this material around the zones to be worked. One can distinguish a few of them on the side of the face and on the neck. He then applied flattened pieces of different thicknesses on the back and sides of the head.

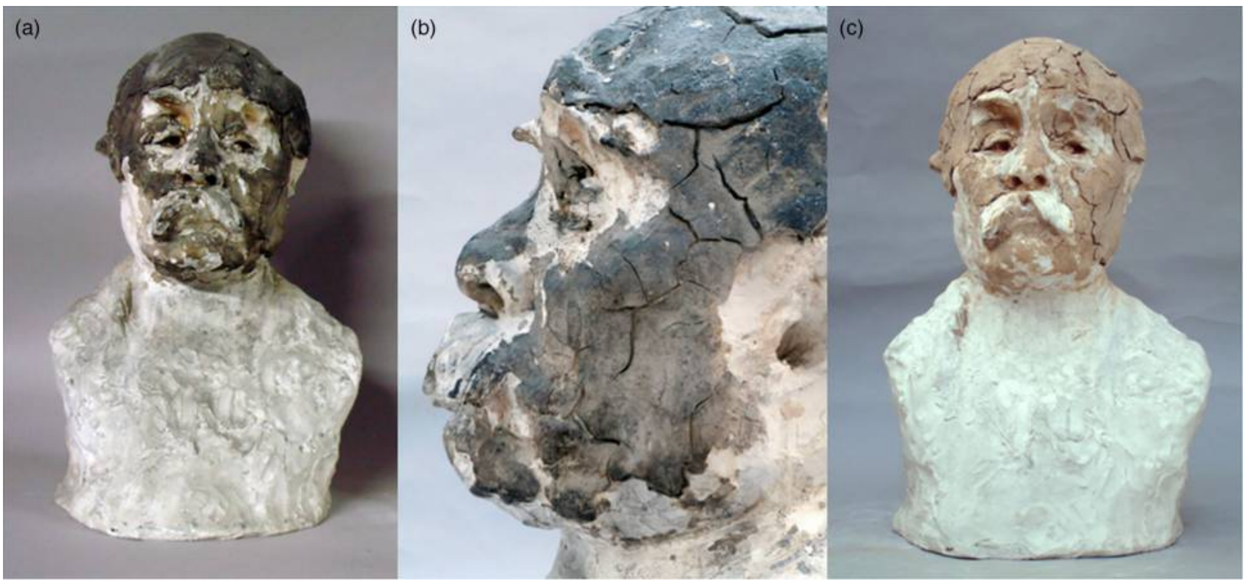


**Figure 2** ***Clemenceau, bust*** **(S.01982, Musée Rodin, height: 50 cm, length: 34 cm, width: 32 cm). (A) Before conservation; (B) detail from** ***Clemenceau bust*** **showing cracks and dirty surface of the modeling material; (C) after conservation. Photo credits: H. Bluzat, A. Cascio, and G. Mary.**

Before conservation, the bust displayed a very heterogeneous aspect (Fig. 1A and B). The MMM surface looked like black crusts and contrasted heavily with the very white, though dusty, plaster. The overall appearance was very alarming and the preservation of the MMM fragments was critical.

The bust of *Clemenceau* (Fig. 2) is a model for a portrait ordered by the Argentinean government, in thanks for a series of conferences Clemenceau gave in Buenos Aires in 1909. It is one of the last studies in a long series of at least 30 models. Three of them have been reworked with MMM and two versions of this bust were analyzed in the present work (S.01982 and S.01730). The techniques used and the state of conservation are similar to those of the *Hanako* head. The plaster of the bust of *Clemenceau* (S.1982) was heavily reworked with raps and chisel in order to create space for the modeling volumes and to improve adherence of MMM. This latter material was added to emphasize the expression of the face. Its surface also presented black crusts but thinner than those found on the head of *Hanako*.

A survey of the entire museum's collection showed that the use of such MMM is quite widespread in Rodin's work. At least 60 sculptures incorporating this material emerged through a preliminary examination of several hundred models. Although beeswax-based modeling materials have been documented for Rodin, they are not the focus of this work. MMMs were used on plaster models which represent important intermediate steps in the creative process of Rodin's works of art. These models led to the definitive models used for the production of commissioned bronze or marble sculptures. Rodin added MMM in localized areas to accentuate details or to modify volumes. He could also modify certain forms by applying it in thick, sometimes large sheets, as in the case of *Hanako* and *Clemenceau* (Figs. 1 and 2).


**Figure 3 Two examples of the use of MMMs in Rodin's work. (A) As the main component, in *Head of Balzac* (S.00265, Musée Rodin, height: 14.7 cm, length: 13.2 cm, width: 11 cm); (B) to hold fabric in place, in *Death* (*La mort*; S.02301, Musée Rodin, height: 29.5 cm, length: 29.8 cm, width: 26. 2 cm) (highlighted with an arrow). Photo credits: C. Barajan for '(A)' and H. Bluzat, A. Cascio, and G. Mary for '(B)'.**

If one considers the entirety of Rodin's plasters, the use of MMM remains modest compared to that of clay. Rodin had a preference for using clay to make his models, and, in general, to develop his creative work process. Malleable MMM, however, allowed him to continue his work on plaster pieces. Unlike clay, such MMM could be reworked without drying and would adhere well to plaster. Accordingly, the use of MMM was of paramount importance, offering to Rodin the possibility to rework, several times, and without time constraints, specific parts of his works. The final work could then be molded, without any risk of deformation. Due to their intrinsic plastic and non-drying properties, MMM offered Rodin new possibilities to further develop his art.

In addition to these localized uses on plaster sculptures, MMM was sometimes used alone, to produce a full model, like for *the Head of Balzac* (S.00265) (Fig. 3A). It was also employed to hold paper or fabric in place, as in the case of sculpture of *Death* (*La mort*; S.02301) (Fig. 3B).

As seen through these different examples, most of these sculptures present damages. Considerable shrinkage of the MMM affects the objects, involving cracks on the surface, and lifting or detachment of large flakes. This shrinkage also creates spaces between the plaster and the MMM or within the material itself. The material has become rigid and brittle. The slightest pressure provokes loss of the fragments as observed on *Half-length figure of a woman* (*Figure de femme à mi-corps*, S.06583) (Fig. 4A and B) or on *Child with body barely modeled* (*Enfant au corps à peine modelé*, S.00303). The weight and size of the fragments and flakes varies, going up to approximately 300 g in weight and 10 cm in length. These uplifted areas and loss of adhesion occur almost always at the junction of the plaster and the MMM. These phenomena are favored by the particularly porous character of the plaster. Areas showing recent losses of MMM exhibit a very distinct yellow coloration and a greasy texture. These changes in aspect suggest that the physical and chemical properties of the underlying plaster have been altered.

The deposits observed on the surface of the MMM (Fig. 1B on *Hanako* and Fig. 2B on *Clemenceau*) can be of a different nature according to each case: either in fine layers, a simple deposit of dust favored by the very electrostatic and slightly sticky character of the MMM, or in thicker layers that seem closer to a crust. The aspect of this crust is gray, rough, and in some areas so thick that it has a tendency to detach.

### *History of MMMs*

Studies of historical use of modeling material in sculptures have been already reported (Reau, 1930; Colinart

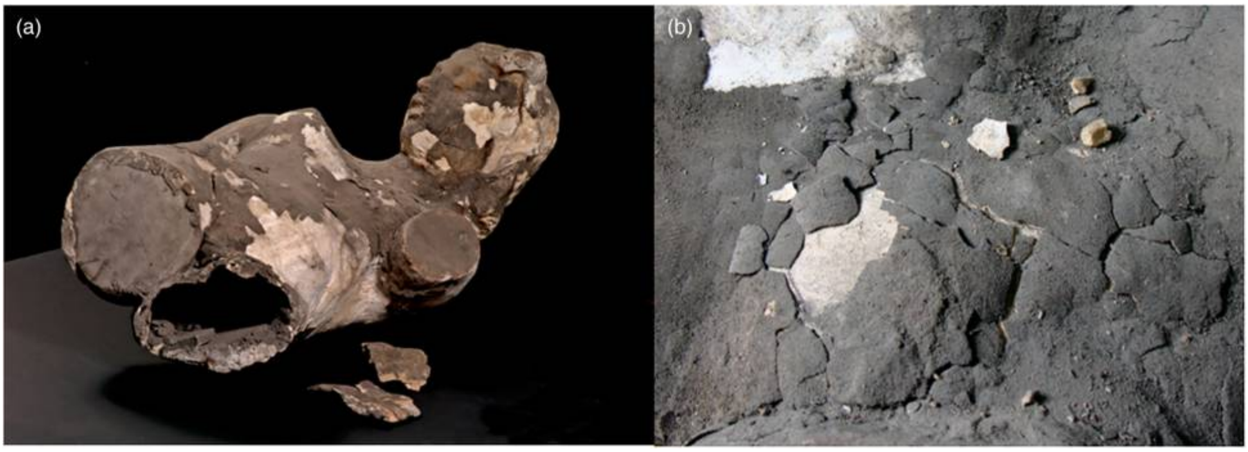


**Figure 4 Example of alteration by loss of the fragments in (A) *Half-length figure of a woman* (*Figure de femme à mi-corps*; S.06583, Musée Rodin, height: 78 cm, length: 46 cm, width: 38.5 cm); (B) detail of the breast shows flaking of dusty modeling material on core plaster. Photo credits: C. Barajan for '(A)' and H. Bluzat, A. Cascio, and G. Mary for '(B)'.**

*et al.*, 1987; Mills & White, 1994; Regert *et al.*, 2005, 2006; Lattuati-Derieux *et al.*, 2008; Berrie *et al.*, 2010; Gramtorp *et al.*, 2015). Traditionally, clay or waxy natural materials, such as beeswax, were often used for sculpture, especially during the nineteenth century. Some additives, such as minerals, starch, or pine resin, could also be mixed with these waxy materials in order to change the physical properties or aspect (Colinart *et al.*, 1987; Regert *et al.*, 2005; Berrie *et al.*, 2010; Gramtorp *et al.*, 2015). At this time, however, some alternative synthetic materials introduced new formulations for modeling materials. They were made with substances coming from the exploitation of petroleum products, like paraffin (isolated by Reichenbach in 1830 and commercialized around 1850), from products of vegetal origin, such as Japan wax, or from hydrolysis of animal fats (a process described by Chevreul in 1823), such as stearin (Chevreul, 1823; Colinart *et al.*, 1987; Regert *et al.*, 2005).

More precisely, Moins gives an interesting overview of the 'invention' of MMM (Moins, 2001). Two compositions were described, by two persons, in Southern Europe and Northern Europe, almost simultaneously at the end of the nineteenth century. In Italy, Tschudi formulated a new material, named *Plastiline*. It was made of kaolin and native sulfur mixed with lanoline or glycerin. In England, William Harbutt (1844–1921) created in 1897 a MMM called *Plasticine* based on undefined waxy material and oil, which can be mixed to pigments. These two new MMMs provided at this period an alternative to beeswax, known since antiquity.

Today, different names are used to designate such modeling materials, such as *plasticine* (in UK, USA, and Belgium), *plastiline* or *plastilina* (in France and Italy). Sometimes the terms *plastaline*, *plastelline*, *plasteline*, *Plasteïne*, and *plastilene* are also used (Moins, 2001; Berrie *et al.*, 2010). Whatever the writing, these different names with an 'l' and not a 'c' do not necessarily refer to the original Tschudi's *Plastiline*. In France, the term *Plastiline* is often overused and, from one reference to another, definitions vary. The term actually encloses all modeling materials despite the fact that *Plastiline* is only one type of many.

### *Implementation of a protocol for chemical characterization*

Taking into account the various possible compositions of these MMMs, it was of interest to get a clear identification of the organic and inorganic ingredients constituting the MMMs used by Rodin. Gas chromatography has already demonstrated its potential for the characterization of the organic components present in various MMMs (Regert *et al.*, 2005, 2006; Berrie *et al.*, 2010) and it was applied here similarly. Fourier transform infrared (FTIR) spectroscopy, X-ray diffraction (XRD) spectrometry, and visible and electron microscopies were also employed, in particular for the identification of mineral phases.

In addition to the determination of the composition, additional analyses were undertaken to determine the composition of altered areas of the MMMs. The previous techniques were combined with synchrotron radiation (SR)-based analyses. These methods are increasingly used in the field of cultural heritage (Bertrand *et al.*, 2012). 2D micro-X-ray fluorescence (μXRF) and μFTIR were carried out to identify and locate the main components in both the original and the degraded regions in order to get information about degradation processes.

### *Implementation of a protocol for conservation*

Regarding the conservation treatment, the first goal was to stop the loss of fragments and flakes of MMM and to obtain an aspect as close as possible to the original one. The difficulty of this task lies in finding an efficient and compatible adhesive that ensures adhesion between the very hydrophilic plaster and the rather hydrophobic MMM. Certain alterations, such as cracking and deformations, have an irremediable character that cannot be ameliorated. This study aimed at recovering the original ivory color of the MMM and especially at attenuating the contrast of its black aspect with the white plaster. The major challenge regarding cleaning was to conserve even the smallest and most detailed traces of tools and fingerprints observed on this soft material (Fig. 1B).

## Materials and methods

### *Corpus of objects and of fragments sampled for chemical characterization*

Out of 60 sculptures showing the use of MMM in the Rodin museum collection, 35 were chosen for the macroscopic observation of uses of MMM and of their alterations. Among these different objects, 12 were selected for further chemical study of their composition and alteration, through a multi-analytical approach. Micro-sampling (less than $1 \times 1 \times 1$ mm$^3$) was performed with a scalpel under binocular magnifier and the samples were stored in glass containers. Different areas were selected to represent different colors, uses, and alterations, which are summarized in Table 1. Each sample was then divided into two parts on a glass slide after preliminary observation with a stereo microscope. One part was retained for FTIR, XRD, and gas chromatography fitted with flame ionization detector (GC–FID) or coupled with mass spectrometry (GC–MS).

The other was embedded in a polyester resin (Sody 33 with catalytic agent Sody 33 C), wet ground, and dry polished with Micro-mesh (final step 12 000 mesh) to prepare cross-sections. They were studied with stereo microscopy, staining tests, and scanning electron microscopy–energy dispersive X-ray spectrometry (SEM–EDX).

SR μFTIR and μXRF were performed on samples from a sculpture which presented several patterns of surface alterations: *Two figures embraced on a pillar* (*Deux figures enlacées sur un pilier*, S.05703). In addition to the embedded and polished cross-sections prepared as described above, some 10 thin sections were sliced from MMM fragments with a scalpel and pressed between two diamond windows.

Details of experimental conditions for chemical characterization and list of materials are provided in Appendix.

In parallel to the analysis of samples from sculptures, mock-ups were prepared in order to carry out conservation tests. Those tests were intended to help determine the best-suited conservation materials and techniques of cleaning and consolidation. Due to the time constraints of a conservation action prior to an exhibition, the mock-up samples were limited to only one type of MMM, the ivory-colored one observed on the *Clemenceau* and *Hanako* busts. Mock-ups were realized with a similar MMM, Plastiline® no. 50. Even if Plastiline® no. 50 does not have exactly the same characteristics as the aged MMM (see details below in Section 'Results of the conservation tests'), it was the closest commercial product among those available on the market that were tested for this study.

### *Tests and methodology for the conservation treatment*

pH measurements were taken with a compact pH meter (Horiba TwinpH 212) following the procedure developed by Wolbers (Larochette, 2012). A small piece of blotting paper dampened with deionized water was applied on the MMM for one minute, removed, and placed on the sensor of the pH meter (Delidow & Albertson, 2010). Determining the pH of water-extractable materials at or near the surface of the modeling material allowed us to choose the conservation products and formulate them, especially adhesives, with a similar and compatible pH.

Solubility tests were carried out in order to determine the sensitivity of the MMM to solvents potentially used in cleaning and consolidation processes. Samples of Plastiline® no. 50 were weighed (1 g) and then placed in sealed test tubes with different solvents: demineralized water, ethanol, acetone, ethyl acetate, and ligroin (a petroleum ether). Though it was already expected that ligroin solubilizes the components of Plastiline®, it was decided to test it as a comparison to other solvents. In order to have the most reliable results, each sample was tested twice. Immersion tests were carried out after 10, 30, 60, and 120 minutes. An ultimate weighting was made after 24 hours to observe degradation features. Although 24 hours represent an intentionally excessive (and unrealistic) exposure to solvents, it could still be representative of a situation when the solvent is adsorbed in the micro-porosity of material. After immersion, the 10 samples were drained and weighed. Finally, after two weeks of drying in air, samples were weighed again, to observe any possible impact of solvent evaporation. In practice, for the actual conservation procedures, the treatment products were applied only on the surface and for no longer than two hours.

Bonding tests aimed at finding glues which would ensure the bonding of broken MMM fragments to the plaster. The Plastiline® no. 50 was sliced into disks of varying thicknesses, conserving the initial cylindrical form of the packaging tube (5.5 cm diameter), in order to obtain a large range of samples weighing from 10 to 300 g each. Tablets of Molda3® plaster were made (carefully mixed without the presence of air bubbles and without the addition of mold-release agents) as a model of plaster in Rodin's sculptures. Even if it is usual to seal or consolidate the plaster

**Table 1 List of studied sculptures from which samples were taken, and summary of chemical analyses and macroscopic observations**

| Title and inventory number | Materials | Date | Group | Color | Use | Alterations |
|---|---|---|---|---|---|---|
| *Child with body barely modeled* (*Enfant au corps à peine modelé*) S.00303 | Terracotta and MMM* | c. 1880 | Beeswax and starch | Dark brown | Addition of small sculpted volumes | Lack of adhesion, loss |
| *Standing embracing couple* (*Couple enlacé*). S.02723 | Plaster and MMM | ? | #1 Zinc oleate + native sulfur + mineral filler | Gray | Addition of small sculpted volumes | Shrinkage, detached fragments |
| *Head of Balzac* (*Balzac*, *étude de tête*) S.00265 | MMM | c. 1897 | #1 Zinc oleate + native sulfur + mineral filler | Brown ocher | sculpting | Surface deposits, fine layer of dust |
| *Young girl disclosing her secret to Isis* (*Jeune fille confiant son secret à Isis*) S.03464 | Plaster and MMM | c. 1895–1900 | #2 Paraffin + fatty matter + filler ($CaCO_3$) | Ivory | Attaching additional parts | Shrinkage, small protrusions |
| *Death* (*La mort*) S.02301 | Plaster and MMM | probably c. 1898 | #2 Paraffin + fatty matter + filler | Ivory | Addition of small sculpted volumes | Shrinkage, loss, protrusions, efflorescences, thick black crusts |
| *Two seated nude women* (*Deux, Nus féminins assis*) S.02580 | Plaster and MMM | c. 1895–1900 | #2 Paraffin + fatty matter + filler | Ivory | Addition of small sculpted volumes | Shrinkage, loss, cracking, protrusions, efflorescences, thick black crusts |
| *Two figures embraced on a pillar* (*Deux figures enlacées sur un pilier*) S.05703 | Plaster and MMM | c. 1900 | #2 Paraffin + fatty matter + filler | Ivory | Addition of small sculpted volumes | Shrinkage, loss, cracking, protrusions, efflorescences, thick black crusts |
| *The Whistler Muse* (*Muse Whistler*) S.02452 | Plaster and MMM | 1907–1908 | #1 Zinc oleate + native sulfur + mineral filler | Brown ocher | Addition of small sculpted volumes | Surface deposits, fine layer of dust, detached fragments |
| *Hanako* (*Hanako*) S.02242 | Plaster and MMM | probably c. 1908 to - 1912 | #2 Paraffin + fatty matter + filler | Ivory | Addition of large sculpted volumes | Shrinkage, loss, cracking, protrusions, efflorescences, thick black crusts |
| *Half-length figure of a woman* (*Figure de femme à mi-corps*) S.06583 | Plaster and MMM | c. 1910 | #2 Paraffin + fatty matter + filler | Ivory | Addition of large sculpted volumes | Shrinkage, loss, cracking, protrusions, efflorescences, thick black crusts |
| *Bust of Clemenceau* (*Buste de Clémenceau*) S.01982 | Plaster and MMM | 1911–1913 | #2 Paraffin + fatty matter + filler | Ivory | Addition of large sculpted volumes | Shrinkage, loss, cracking, protrusions, efflorescences, thick black crusts |
| *Bust of Clemenceau* (*Buste de Clémenceau*) S.01730 | Plaster and MMM | 1911–1913 | #2 Paraffin + fatty matter + filler | Ivory | Addition of large sculpted volumes | Shrinkage, loss, cracking, protrusions, efflorescences, thick black crusts |

*MMM, modern modeling material.

surface before gluing, this step was not done on the plaster tablets. Indeed, this would have not been applicable on the busts of *Clemenceau* and *Hanako* due to the presently greasy surface of the plaster and limited access to it because of the residual MMM still attached. The adhesion criteria were: affinity with both the plaster and the MMM; reversibility; stability; similar pH to both (±2); flexibility; high viscosity; and efficient adhesive properties to fix a mass of approximately 300 g. These criteria led to the selection of five adhesives for testing, two emulsion adhesives in water (Vinavil® 59 and Plextol® B500, without dilution) and three solution adhesives (Paraloid® B-72 diluted in ethanol/acetone at 30% w/w, Paraloid® B-44 diluted in acetone at 40% w/w, and Pioloform® BM18 diluted in ethanol at 30% w/w). They are characterized by vinylic group (Vinavil® 59 and Pioloform® BM18) or acrylic group (Plextol® B500, and Paraloid® B-72 and B-44) and were chosen out of a selection of widely tested conservation products. The emulsions were used pure. The five adhesives were always applied in the same manner and amount. Three milliliters was placed in drops on the surface of the Plastiline®. The samples of Plastiline® were applied by hand, with little pressure, on the top horizontal side of the plaster tablets. After a drying period of 48 hours, the mock-ups were placed vertically in order to test the shear of the bond on mock-ups of Plastiline® of increasing weight. For more reliable results, all mock-up samples were prepared twice.

Some other tests were performed to choose the most suitable product for consolidation of the MMM flaking from the surface of the plaster. These tests were designed to reproduce the case where lifted fragments were still attached. The surfaces intended to receive the adhesive were not directly accessible, and the adhesive was therefore injected by syringe. The criteria for selection were similar to the ones for adhesive tests. In addition, viscosity and a mat aspect were important factors. Fillers might also be added to modify the adhesives' viscosity when necessary. Plastiline® test samples in the form of small disks were prepared by cutting out identical pieces of a layer of flattened Plastiline® (measuring 2 mm in thickness), weighing approximately 10 g each. The small disks of Plastiline® were applied, without pressure, on the plaster tablets prepared as previously described for bonding adhesive tests. The upper edges of the disks were lifted up. Seven adhesives were tested: Paraloid® B-72; Pioloform® BN, BM, and BL18 (diluted in ethanol at 5, 10, and 20% w/w); and Vinavil® 59, Plextol® B500, and Primal® E330S (diluted in water at 5, 10, and 20% w/w). Pioloform® BN, BM, and BL18 presented short, medium, and long molecular chain lengths, thus offering different viscosities for the same concentration. Solutions were always applied in the same amount and manner. Adhesive (3 ml) was injected by syringe at the junction of the lifted up Plastiline® and the plaster tablet. Different adhesives and concentrations were tested. After a drying period of 48 hours, the test tablets were placed vertically in order to test the shear of the bond induced by the weight of the Plastiline®. Adhesion was also tested by gentle finger pressure on the disk. All mock-up samples were done twice.

Due to the time constraints of conservation prior to the exhibition and also because simulating similar dirt and aging was not feasible, cleaning tests were carried out directly on fragments of MMM detached from Rodin's sculptures. The plaster was cleaned in a traditional way by application of a clay gel composed of attapulgite, carboxymethylcellulose, and cellulose powder (products detailed in the 'List of suppliers'). The areas with MMM were carefully avoided during the cleaning of plaster.

The softness of MMM and its sensitivity to solvents do not permit the action of repeated abrasion with cotton swabs, so laser cleaning was first tested. Considering the strong contrast between the black layer of dirt and the ivory-colored substrate, positive results with laser photo-ablation were expected.

Two types of machines, Artlight II® and Art laser®, were used on the different types of surface conditions of the MMM, dirty or altered. Both are Nd:YAG lasers (1064 mm). The Artlight II® is a small and compact machine; the pulse is adjustable up to 150 mJ, the frequency from 0.5 up to 20 Hz, and the diameter of spot size from 1 to 4 mm. The Art laser® is a larger machine, the pulse is adjustable up to 350 mJ, the frequency range is from a single pulse up to 30 Hz, and the diameter of spot size is adjustable from 1 to 12 mm. In all cases, prior to cleaning, the surface was humidified with water spray in order to minimize the elevation of temperature and to improve the efficiency of the laser. Indeed, lasers work better on dark or black areas. The wetting darkens the surface and this contrast enhances the efficiency of the laser. The temperature of the water could also be a contributing factor.

## Chemical characterization of the micro-fragments

### *Compositions of MMMs: the identification of two groups*

GC–FID, GC–MS, FTIR, XRD, SEM–EDX analyses and visible light microscopy revealed that Rodin used two different types of MMMs, whose compositions are close to the original 'plastiline' and 'plasticine' recipes described in the literature (Table 1).

The first type of MMM (group 1) was found in three sculptures: *Standing embracing couple* (*Couple enlacé*, S02723), *Head of Balzac* (S.00265, Fig. 3A), and *The*

*Whistler Muse* (S.02452). The colors of MMM from this group present multiple shades from brown ocher (Fig. 5A) to gray. It is made up of fatty matter (animal or vegetable, but most probably animal considering the presence of fatty acid containing an odd number of carbons) where the oleic chain is the main component, as determined by GC–MS (Fig. 6B) terminated by a zinc carboxylate group clearly identified by FTIR (Fig. 7A). The homogeneous presence of Zn in the organic matrix was confirmed by µXRF. SEM–EDX also revealed the presence of sulfur and iron. FTIR identified barium sulfates and earths. In addition, as shown in Fig. 5A and B, µXRF and SEM–EDX of the cross-sections showed that sulfur is concentrated in white granules, of about 10 µm diameter. Micro-X-ray absorption near edge spectroscopy (µXANES) at the sulfur K-edge and µXRD allowed identification of these grains as native sulfur (Fig. 7B).

The second type of MMM (group 2) was found on eight works of the selected corpus (cf. Table 1). The color (except in the altered areas on surface) is a uniform ivory hue (Fig. 8A and B, also visible in the cross-section in Fig. 5C). It consists of paraffin and fatty matter (cf. chromatogram in Fig. 6C) filled with calcium carbonate (back-scattered electrons, SEM-BSE in Fig. 5D, µXRF and µFTIR in Fig. 8C).

The two busts to be restored, *Hanako* (S.02242) and *Clemenceau* (S.01982), belong to this group. Of the 60 sculptures containing MMM, 41 presented such an ivory color, and could be tentatively assigned to this group.

Similar to what was found in group 1, the presence of native sulfur in MMM has already been mentioned. In 1878, Giesel details the composition of 'Plastilina' as sulfur, zinc carboxylates (from oil), unsaponified oil, some wax, and clay (Giesel, 1878). The nature of wax (natural or mineral) is not specified. These ingredients correspond well to those found in Rodin's sculptures (group 1). Three publications recently reported the use of such sulfur-based MMM, and underlined the risks associated with corrosion reactions when sulfur is in contact with metallic artifacts. Both Rolfe (1999) and Berrie *et al.* (2010) mentioned the corrosion of internal metal armatures in some sculptures by Degas. Eggert reported a mediaeval bronze fibula developing 'black spots' of copper sulfide after a nine-year exposure to a sulfur-based MMM in a display case (Eggert, 2006).

Finally, in one sculpture of the selected corpus, *Child with body barely modeled* (*Enfant au corps à peine modelé*, S.00303), a completely different composition was found. This red modeling material is composed of beeswax (Fig. 6A) mixed with starch and iron oxides (the phthalate peak visible in Fig. 6A is a common artifact in our GC analyses). The limited occurrence of this beeswax-based material in our study is to be related to the selection of samples made in the museum's collection within the scope of the current study, which was focused on MMM and not beeswax-based modeling material. It is therefore not representative of the use of beeswax by Rodin through time. Indeed,

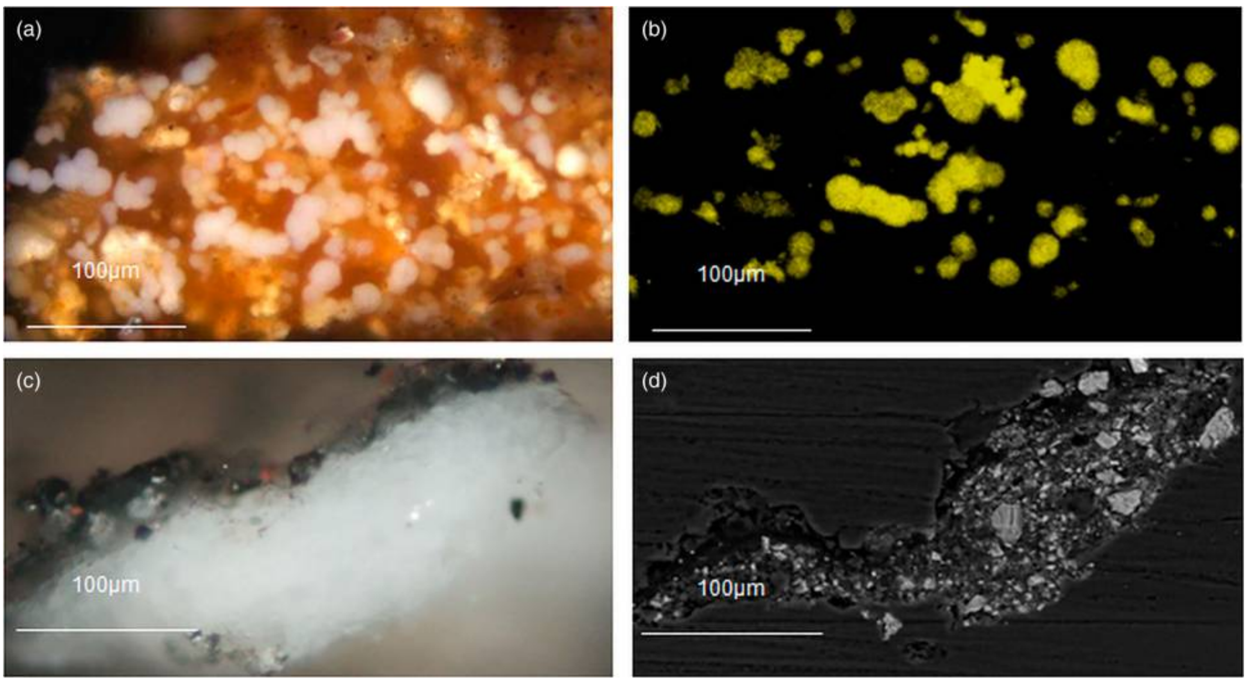


**Figure 5 Visible light and electron microscopy of cross-sections of fragments from a sculpture. (A) and (B) from group 1 (*Head of Balzac*, S.00265): (A) visible light microscopy, (B) sulfur map by SEM–EDX; (C) and (D) from group 2 (*Standing embracing couple*, S02723): (C) visible light microscopy and (D) SEM backscattered electron image. Photo credits: C2RMF.**

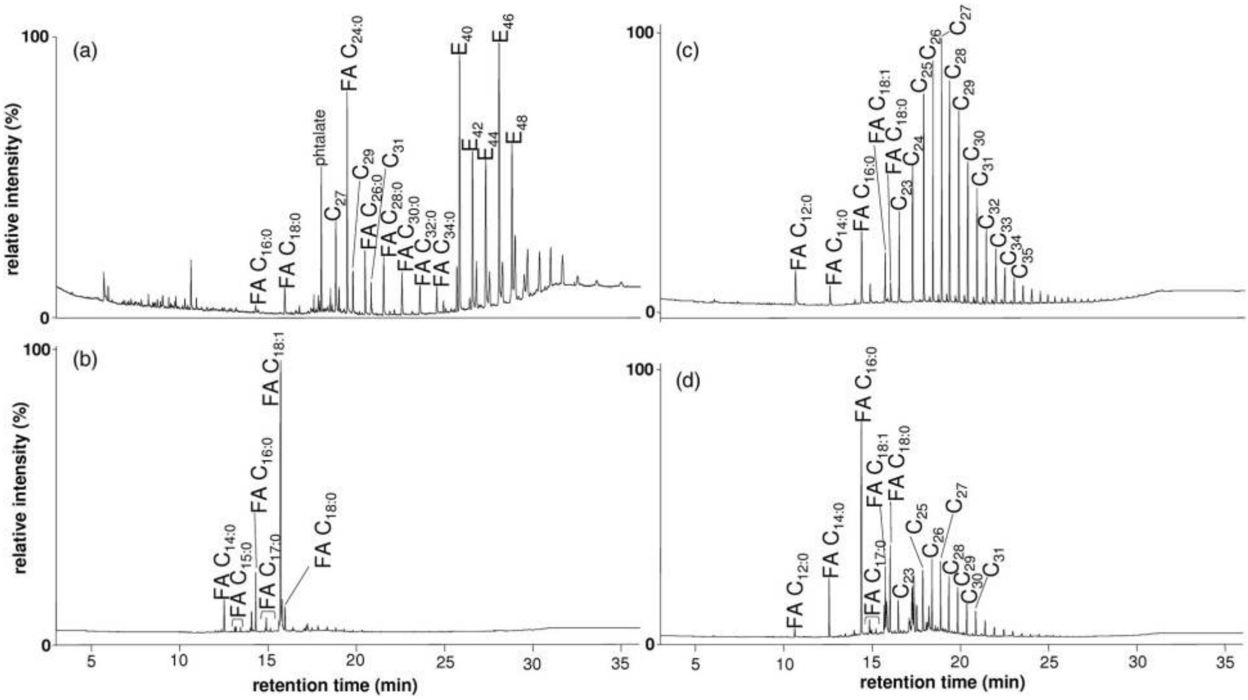

**Figure 6 Chromatogram of modeling material taken from the sculptures studied: (A) from *Child with body barely modeled* (*Enfant au corps à peine modelé*, S.00303); (B) from group 1 (*Standing embracing couple*, S.02723); (C) and (D) from group 2 (*Two figures embraced on a pillar*, S.05703): (C) sampled in the internal ivory-colored modeling material and (D) sampled in superficial yellow patina (cf. Fig. 8A). Linear alkanes, fatty acids, and palmitate esters are, respectively, labeled $C_x$, FA $C_{x:n}$, and $E_x$ (with *x* and *n* corresponding, respectively, to the number of carbons and the number of unsaturated bond in the linear chain). Photo credits: C2RMF.**

this type of composition has already been identified on the sculpture *Sleep* (*Le Sommeil*) (Colinart *et al.*, 1987) and many other examples of use of this type of material by Rodin and other artists are known, frequently mixed with pine resin. For example *Bust of Aline* by P. Gauguin (1882), *Art Criticism* (*La Critique Artistique*) by F.R. Carabin (1896) (Regert *et al.*, 2006), *Miner from the Loire* (*Le Mineur de la Loire*) by J.-J. Carriès (1886) (Lattuati-Derieux *et al.*, 2008), as well as a corpus of 15 sculptures by *Gustave Moreau (1826–1898)* studied in 2009 at Centre de Recherche et de Restauration des Musées de France (C2RMF) prior to an exhibition (Forest, 2010).

Some general ideas can be drawn from the complete corpus by comparing the date of the models and the composition of the materials. Works analyzed for this study date from the 1880s to 1913 (Table 1). The earliest uses of MMM on the plasters sampled date from 1895. Therefore Rodin had experimented very quickly with the newly available MMM. The analytical results do not reveal any chronological difference in the use of group 1 and group 2 MMM, or show any direct link between the composition of the MMM and their use. The materials used for modeling belong as much to group 1 as to group 2. Also, the group 2 material is used as much for modeling and fixing paper or fabric to the sculpture as for completing models used for reproduction with the use of a pointing machine.

### *Characterization of deterioration and alteration products of group 2*

The alterations observed do not seem directly linked to the type of application of the MMM. Whether the volumes are applied in thick masses or in thin layers, they are not less cracked or less adherent. Conversely, the morphology of these alterations seems linked to the composition of the modeling material used (Table 1).

For example, shrinkage of the material in a compact mass is characteristic of group 1. Cracking, flaking, and thick black crusts on the surface are characteristics of group 2 (Figs. 1B, 2B, and 4B). The MMM of group 2 shows the highest amount of degradation (shrinking, black crust) thereby putting the preservation of the concerned artwork at risk.

For *Hanako* and the two *Clemenceau* busts (S.01730 and S.01982), based on the GC–MS analyses, the black crust is not fundamentally different from the core matter but shows higher concentrations of alkanes from paraffin than of fatty acids from fat, in a converse ratio to that observed in the core matter. The loss of fatty acids (acting as plasticizers) decreases material flexibility, causing cracking and loss of fragments. This may correspond to a migration of the alkanes inside the MMM or to a loss of fatty acids on the surface, as has already been noted in the case of wax sculptures (Regert *et al.*, 2001).

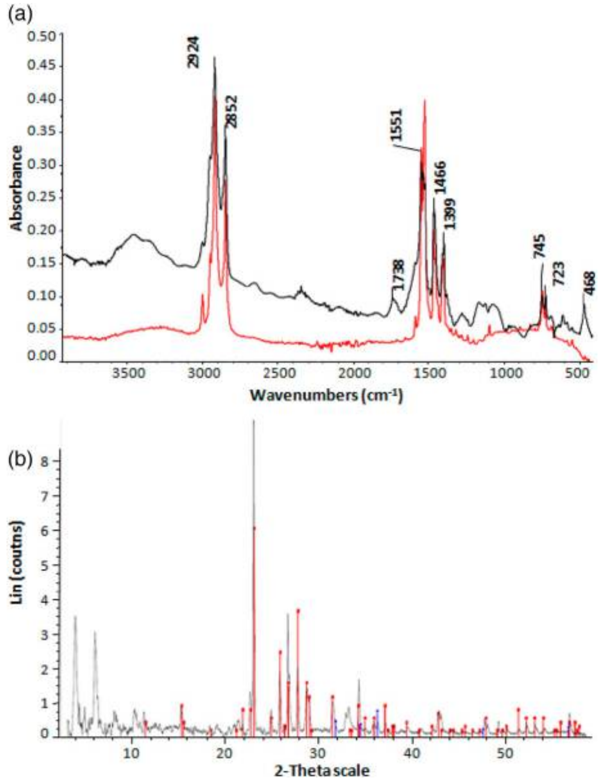


**Figure 7 Chemical characterization of a fragment from *Standing embracing couple* (S02723). (A) By FTIR (the spectrum acquired on the sample, in black, is superimposed with the one acquired on a reference of zinc oleate, in red. The triplet in the region 1560–1380 cm$^{-1}$ is characteristic of a zinc carboxylate group). (B) By XRD. The main peaks are attributed to native S (in red, peaks given for reference 00-008-0247 (I) - Sulfur syn - S - Y: 53.47% - d x by: 1. - WL: 1.5418-0). The presence of ZnO (in blue, 00-036-1451 (*) - Zincite syn - ZnO - Y: 6.14% - d x by: 1. - WL: 1.5418-0) cannot be excluded. Photo credits: C2RMF.**

The MMM of group 2 present on *Two figures embraced on a pillar* (*Deux figures enlacées sur un pilier*; S.05703) has a yellow shiny superficial patina, sometimes appearing gray or black due to the additional presence of dust (Fig. 8A and B). These different features largely cover the surface of the MMM. Some fragments also exhibit small protrusions (roughly 1 mm in height), white or yellow, contrasting greatly with the superficial black coloration (Fig. 9A and B). A more in-depth study of these various degradations was therefore undertaken.

The GC–MS analyses of the yellow patina show a much higher concentration in fatty acids (Fig. 6D) with respect to the internal composition (Fig. 6C), which would explain the shiny, 'fatty' aspect of the patina. This result differs from those observed on the surface of the two busts of Clemenceau. It also explains the difference of surface appearances in these different sculptures. A similar migration of fatty chains, exuding at the surface of Degas' sculptures, has already been reported (Berrie *et al.*, 2010).

Bulk FTIR analyses of degraded areas (sampling both the yellow patina and some protrusions) revealed the presence of carboxylates and more specifically calcium carboxylates. Such organometallic compounds are sometimes observed in paintings, as small aggregates, called 'protrusions', forming with time by a reaction between the oil binder and metallic compounds. These protrusions are sometimes large and strong enough to disrupt the upper paint layer like small volcanoes (Cotte *et al.*, 2007). In paintings, metallic carboxylates can also be introduced voluntarily in order to modify the physical properties (plasticity, drying, etc.) of the paints (Cotte *et al.*, 2006).

Metallic carboxylates are also regularly used in the plastics industry, due to their various properties (e.g. acid scavengers, lubricants, release agents, etc.). In MMM such as Plasticine®, soaps can be introduced to modulate the viscoplastic rheological behavior of the paste (Raut *et al.*, 2008). As seen above in group 1, carboxylates can represent the main component of some modeling paste. Accordingly, a more in-depth study of the protrusions, their migration, and coloration was undertaken.

Considering the strong heterogeneity associated with these degradations, we decided to carry out dedicated micro-imaging studies using SR-based techniques. The aim was to analyze specifically both the internal regions of the MMM as well as the altered surfaces. Such imaging approaches can provide clues that can lead to a better understanding of the diverse phenomena of degradation. For example, they can help highlight the possible role of an exogenous material (environmental pollutant) as well as the migration and reaction of original ingredients.

Figure 8C shows a combined μFTIR–μXRF analysis of the yellow patina covering the ivory-colored MMM (S.05703). The white/yellow bilayer was slightly distorted during compression with diamond cells, but is still visible (Fig. 8B). A few elemental and chemical maps are presented, illustrating the main trends observed. The yellow coloration is essentially composed of calcium carboxylates. These carboxylates can be easily identified since their FTIR spectrum presents a characteristic doublet at ~1578 and 1542 cm$^{-1}$. The CH stretching bonds (at ~2950 and ~2920 cm$^{-1}$) are characteristic of fatty chains, in agreement with GC–MS results. Other carboxylates are also present (single peak shifting from ~1574 to ~1558 cm$^{-1}$) that could correspond to sodium, magnesium, or potassium carboxylates. Zinc was not detected by SEM–EDX, therefore the presence of Zn carboxylates is not considered relevant for group 2.

Interestingly, all the different carboxylates are present in the yellow patina, but in different areas. They are also detected in the gray upper area. The main difference between yellow and gray layers is the additional presence of aluminum, silicon, and potassium in the gray areas (easily attributable to dust). The

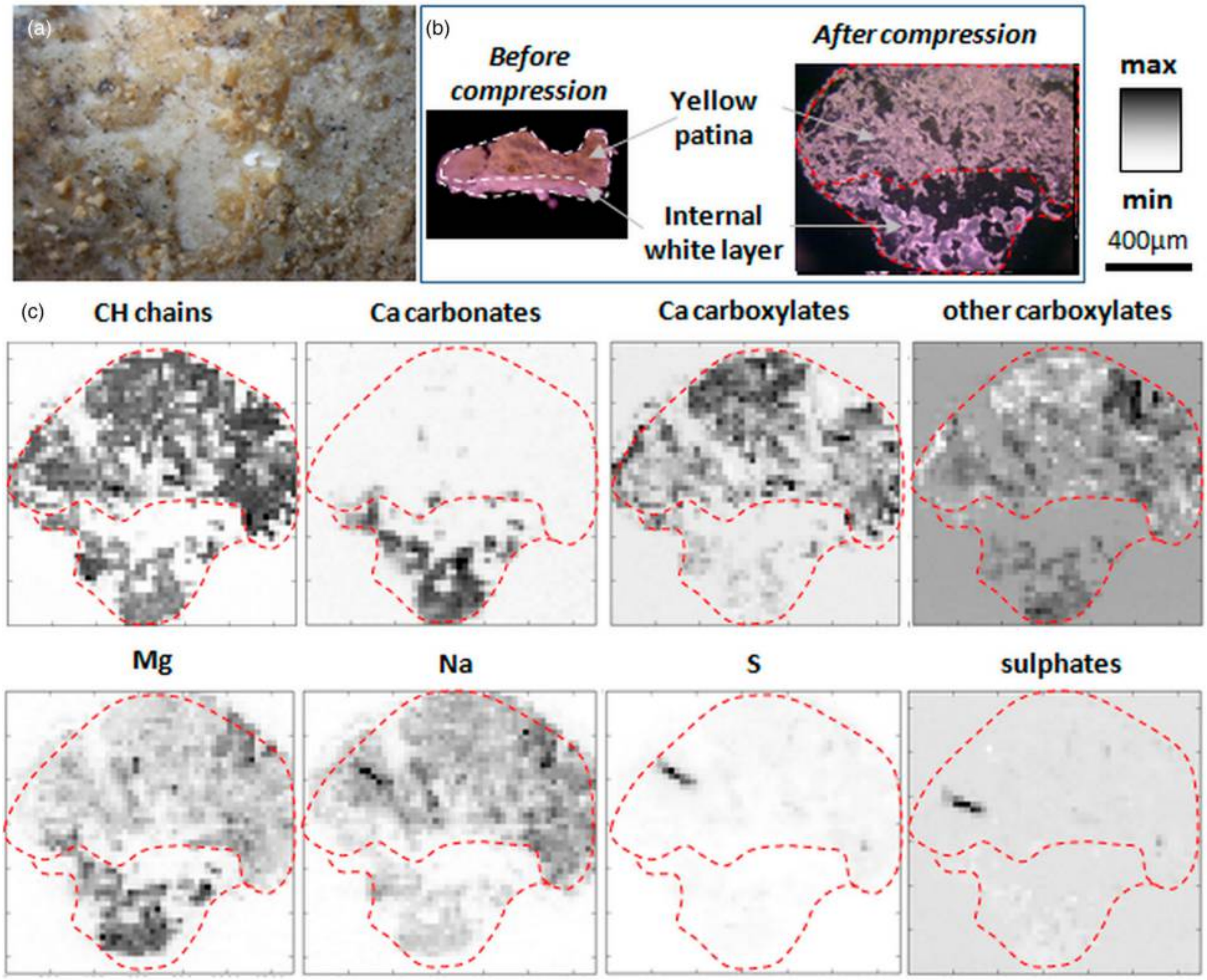


**Figure 8** µXRF and µFTIR analyses of the yellow layer covering the white MMM, on a sample from *Two figures embraced on a pillar* (*Deux figures enlacées sur un pilier*; S.05703). (A) The visible picture on the top left shows the different degradation features (yellow efflorescence, yellow and gray colorations on the original ivory-colored MMM). (B) The sample was prepared by compression between two diamond windows, without any embedding. (C) The maps of CH chains, calcium carbonates, carboxylates, and sulfates were obtained by µFTIR. Elemental maps (Mg, Na, and S) were obtained by µXRF. Photo credits: ESRF.

presence of carboxylates in the internal, white part of MMM is hard to assess by FTIR due to the high absorption of calcium carbonate (large CO band at ~1470 $cm^{-1}$) which may hide the peaks of the carboxylates. They were detected in some fragments. The FTIR analysis of the soluble fraction of the samples shows spectral features similar to sodium or potassium fatty carboxylates (CH stretching bands plus two large bands peaked at ~1564 and 1421 $cm^{-1}$). Calcium carbonates are absent from the upper altered layer. This strongly contributes to the noticeable difference of color.

Figure 9B presents µXRF maps obtained from a protrusion (S.05703). In this case, to better preserve the structure, the sample was embedded and polished. In the cross-section, one can see a thick white layer, corresponding to the MMM, surrounding a darker protrusion. Some gray particles are also observed in the bottom part of the sample. This particular sample was analyzed by µXRF but others were prepared as non-embedded compressed samples for combined µXRF/FTIR analyses. The main observations are summarized here. In protrusions, µXRF mappings reveal high concentrations of sodium and sulfur. µFTIR and µXANES at the sulfur K-edge allow us to identify more precisely sulfates, most presumably sodium sulfates. Sodium and sulfur are concentrated and distributed homogeneously in the protrusions, while they are far less concentrated (a factor of 30) in the thick internal white layer of MMM. Therefore, it seems more probable that the sulfates observed in protrusions come from an external source (possibly the plaster materials present in the vicinity of sculptures). Conversely, while calcium carbonates are highly concentrated in the original white area, they are completely absent from the yellow crusts and the white crystallized protrusions.

In these homogeneous sulfated protrusions, µXRF also detected small magnesium-rich crystals having a rod shape (with a width of a few micrometers and a

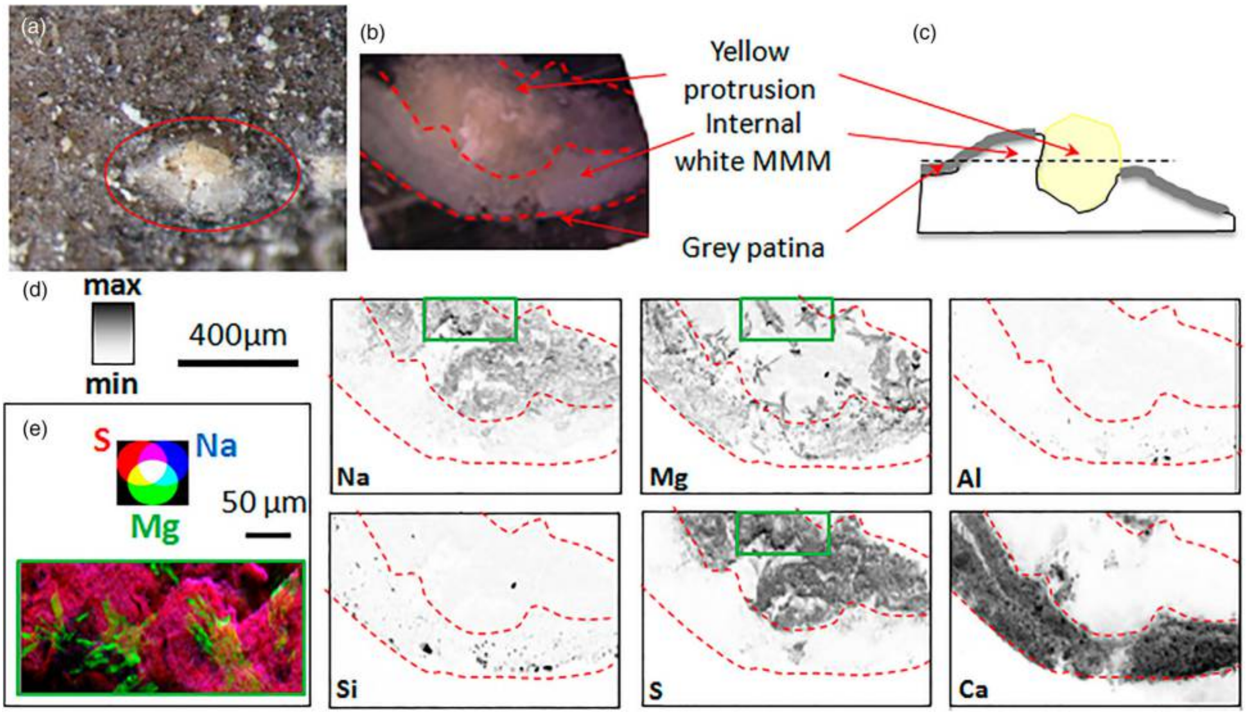


**Figure 9** µXRF analysis of a yellow protrusion from *Two figures embraced on a pillar* (*Deux figures enlacées sur un pilier*; S.05703). Visible image of the protrusion (A) before sampling and (B) after embedding and polishing. Part figure (C) represents a scheme of a virtual cross-section of the protrusion. The dotted line represents the plane along which the sample was polished. (D) µXRF mappings of Na, Mg, Al, Si, S, and Ca. (E) Magnified detail of the Mg crystals (RGB display of S, Mg, and Na). Photo credits: ESRF.

length of a few tenths of a micrometer) (cf. inset in Fig. 9). Magnesium is also detected in the white areas but is present in a more homogeneous, diffuse distribution. The precise type of these magnesium crystals could not be determined so far. µSR–FTIR shows, in addition to the intense signal of sulfates, the presence of long CH chains as well as carboxylates. In GC and GC–MS, the organic phase inside the protrusion appears to be similar to those observed in the white area that can be considered as non-altered zone. In the protrusions, the carboxylate asymmetric stretching band is more in favor of sodium carboxylates (single peak at $\sim$1560 cm$^{-1}$) than of calcium carboxylates.

In conclusion, unlike the carboxylate protrusions observed in some oil paintings, the protrusions here are primarily composed of sulfates. Different carboxylates are present both in the internal part and in the different coloration layers.

Surprisingly, protrusions were not observed in samples from group 1, while sulfur is abundantly present in the bulk material of this group. This observation would support the fact that (i) the sulfur present in MMM group 1 is not prone to oxidation and crystallization, (ii) the sulfates observed in protrusions come from an environmental contamination, and (iii) the crystallization of sulfate-based compounds is strongly connected to the MMM composition. Dedicated experiments of artificial aging of MMM under controlled conditions will be needed to further understand this crystallization phenomenon. In particular, Mg species (in the bulk material and in the protrusions) should be identified to determine if they act as initiators of sulfate aggregation.

## Results of the conservation tests

### *Characterization of Plastiline® no. 50*

All conservation tests were carried out with a specific MMM: Plastiline® no. 50. Its composition was analyzed by GC–FID and showed a bimodal distribution of linear alkanes from *n*C20 to *n*C60 with a maximum around *n*C24 and a secondary lower maximum around *n*C42. This distribution corresponds to those of mineral waxes from fossil matters such as paraffin or ozokerite. Even if it does not contain fatty matter, this composition is more similar to MMM of group 2 than other commercial products analyzed. As this material also contains calcium carbonate as filler, it makes Plastiline® n°50 the best model available for the conservation tests of the two sculptures, *Hanako* (S.02242) and *Clemenceau* (S.01982).

The average pH of several values measured was 7.4 on MMM parts of *Hanako* (S.02242) and *Clemenceau* (S.01982). The pH measurement of Plastiline® no. 50 was 7.5. The plaster of the sculptures on which this material was applied has approximately the same pH. The technical data sheet for the plaster used for the tests specified a pH of 8. The plaster (whose pH was actually measured between 7.5 and 8) tends to become neutral with time by the action of water vapor and carbon dioxide (Delidow & Albertson, 2010).

### *Solubility tests on mock-up samples*

Evolutions of weight after immersion in different solvents are reported in Table 2. Despite a very slight swelling (less than 1%) after immersion in water, the initial weight of the sample was nearly identical after two weeks of evaporation. Tests with all the other solvents showed a loss in weight. There was a noticeable phenomenon of dissolution in different proportions according to each solvent used. The process of solubilization was most noticeable with ligroin: the samples started to dissolve rapidly after their first immersion and they had completely dissolved at the end of the experiment. The samples in acetone and ethyl acetate were partially solubilized; they also whitened and became rigid and fragile (Fig. 10).

As expected, water proved to be the safest solvent tested on modern Plastiline® no. 50. Dissolution of Plastiline in this solvent is negligible. Plastiline® no. 50 differs from the MMM of group 2 by the absence of fatty matter. This matter is usually insoluble in water. Sodium sulfates, sodium, and potassium carboxylates are soluble in water; calcium and magnesium carboxylates are less soluble. $CaCO_3$ is also poorly soluble in water ($K_s = 10^{-8,3}$). Accordingly, water can be considered as a harmless solvent for the treatment of the group 2 modeling material, with limited effect on the body, and some appropriate effects on the protrusions and the fatty patina. However, it is important to keep in mind that these tests correspond to observations made and gathered immediately after the use of water. Without being negligible, as in the case of water, the dissolution of Plastiline in ethanol is minimal. Even though it was not used for cleaning, ethanol could be used as a solvent to dissolve the adhesive.

### *Adhesive tests and treatment*

#### Bonding

The adhesion of Paraloid® B-72 was insufficient to secure samples and Pioloform® BM18 was also unsatisfactory, as the samples came apart just with a light push of the finger. On the other hand, the three other adhesives (Plextol® B500, Vinavil® 59, and Paraloid® B-44) presented signs of good adhesion, with the samples resisting the mechanical stress of a finger-push.

The chemical composition of group 2 MMM (paraffin and fatty matter filled with calcium carbonate) and the solubility test results allowed us to orient our choices towards emulsion adhesives in water.

The absence of starch, which can swell with water, in the chemical composition of group 2 was also allowing deciding factor in the use of this solvent for adhesion.

The choice came down to two adhesives: Plextol® B500 and Vinavil® 59. We chose Plextol® B500 for its superior stability over time. This adhesive is rather runny but it can be thickened with a filler in order to obtain the desired viscosity.

A second series of tests confirmed the efficiency of this adhesive in the bonding of two Plastiline® fragments. This type of intervention was necessary but less frequent than bonding modeling material fragments to plaster.

Bonding was carried out with mixtures of Plextol® B500/Tylose® MH300P (methylhydroxyethylcellulose powder, used as filler or thickener) 70/30, and 50/50 (v/v). The largest fragments were held in place with a slightly elastic cotton bandage that guaranteed a firm upholding without risk of damaging the modeling material.

#### Consolidation of flakes

Paraloid® B-72 and Pioloform® BN18 were not considered because of insufficient adherence: only a small pressure was needed to separate the samples. Plextol® B500, Primal® E330S, and Vinavil 59® displayed satisfactory adherence, with samples resisting mechanical stress.

As previously seen, it is preferable to use water as a solvent, which oriented our choice towards an emulsion adhesive. For a better long-term stability, we preferred an emulsion with acrylic adhesive rather than with vinylic adhesive. Plextol® B500 was preferred to Primal® E330S because it can be used both for bonding and consolidation of flaking modeling material. (Primal® E330S did not have sufficient tackiness for bonding). It also reduced the number of

**Table 2 Evolution of the weight of Plastiline® 50 (in % with respect to time 0) after immersion during *x* minutes in different solvents and after two weeks of drying in air**

| Time (minutes) | 0 | 10 | 30 | 60 | 120 | 1440 | After two weeks of drying in air |
|---|---|---|---|---|---|---|---|
| Water | 0.0 | 0.0 | 0.0 | 0.0 | 0.0 | 0.2 | 0.0 |
| Ethanol | 0.0 | −0.1 | −0.2 | −0.2 | −0.4 | −1.3 | −1.5 |
| Acetone | 0.0 | −0.4 | −0.8 | −1.0 | −1.6 | −4.0 | −5.2 |
| Ethyl acetate | 0.0 | −0.8 | −1.7 | −3.3 | −8.1 | −13.5 | −20.9 |
| Ligroin | 0.0 | −8.1 | −35.3 | −48.7 | Fully dissolved | Fully dissolved | Fully dissolved |

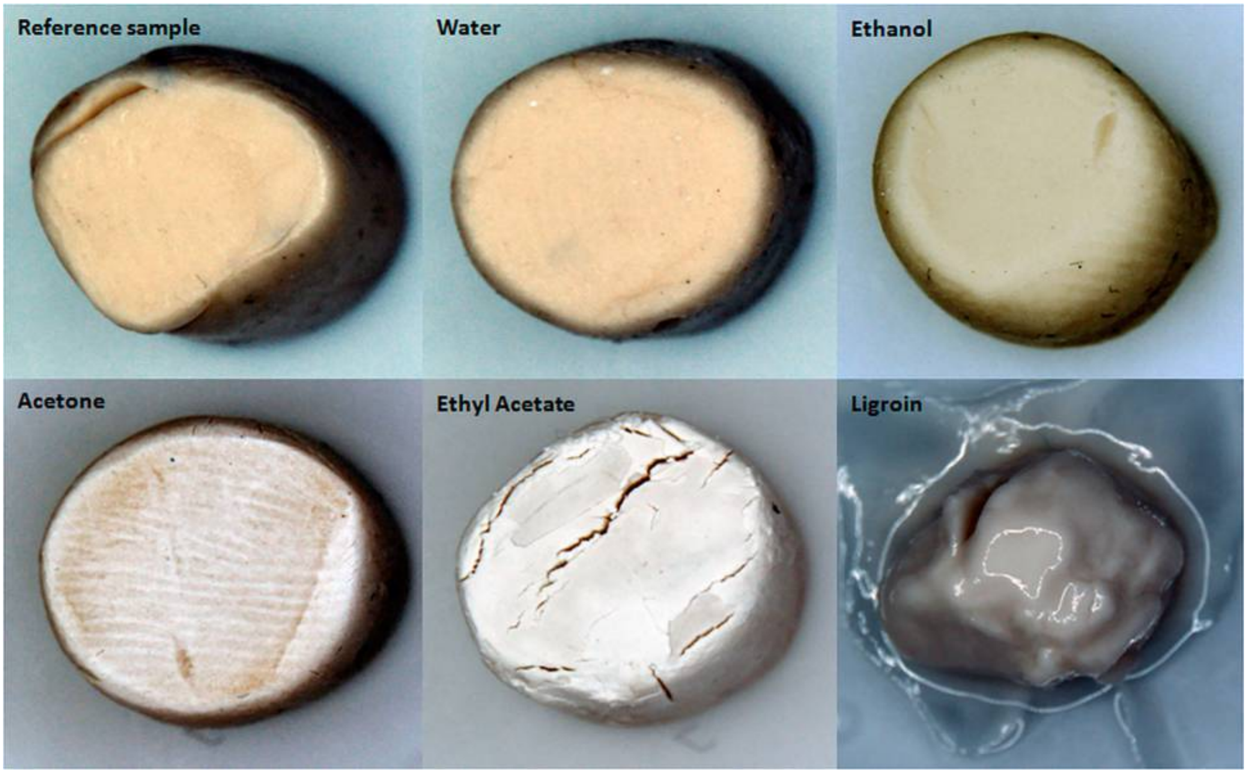


**Figure 10** Solubility test, mock-up samples after one hour of immersion of Plastiline® in several solvents. The reference sample was not immersed in any solvent. Photo credits: C2RMF.

products used in these conservation treatments. Besides having sufficient tackiness, Plextol® B500 can be formulated in a rather fluid state if diluted, or very viscous if fillers are added. This adhesive therefore allowed a wide range of viscosities providing the ability to easily adapt to the different issues present in various areas of these objects. When diluted, the adhesive was liquid enough to be squirted beneath flakes; with fillers, it was sufficiently viscous to form partial fills.

Further tests were done using fillers added to Plextol B500®. When micro-glass-beads (3M Scotchlite® glass beads, twice the amount of filler in volume) or Tylose® MH300P (methylhydroxyethylcellulose, white powder) was added to Plextol® B500, the creamy mixture obtained could not be injected with a syringe. The texture of the mixture Plextol® B500–Tylose® MH300P allowed for bonding and some consolidation of flakes without dripping but shrinkage was observed upon drying. When gap filling was necessary, a mixture with Plextol® B500 micro-glass-beads (which displays no shrinkage after drying) was preferred. After drying, the mixture remained white, whereas the mixture Plextol® B500–Tylose® MH300P presented a translucent appearance. In such a case, the right final color could be obtained by painting the surface.

For the thickest detached fragments it was necessary to create a new link between the plaster and the MMM. To achieve this, a filler made of a mixture of Plextol B500® and micro-glass-beads was used, the latter increasing the viscosity of the adhesive. Due to the very limited access to the altered zones, this adhesive was injected with a syringe.

Another mixture used for the much finer flakes was a mixture of Plextol® B500 and low concentration Tylose® MH300P solution (5% in water), respectively, with the two following ratios 70/30 and 50/50 (v/v). It was injected and the contact between the modeling material and the plaster was achieved with additional slight pressure thanks to small lead-weighted bags. Plextol® B500, pure or diluted in demineralized water (up to 50%), was applied to secure the smallest flakes.

For all reattachment and consolidation operations caution was taken to use controlled pressure as the material was both rigid and brittle (Fig. 11). The surface was cleaned and retouched and finally preventive conservation measures were initiated.

### *Cleaning tests and treatment*

Laser cleaning proved to be a very versatile and useful option in this specific context.

On the dirty, dust covered surfaces, very good results were obtained using the laser at low power (Artlight II® Nd:YAG laser 1064 mm, 8 ns pulse at 100 mJ with 10 Hz frequency). The diameter of the laser spot depends on the laser settings (used in a range between 2 and 4 mm) but also on the distance from the object. The effective spot areas were about 4 mm but were not precisely measured for each cleaning

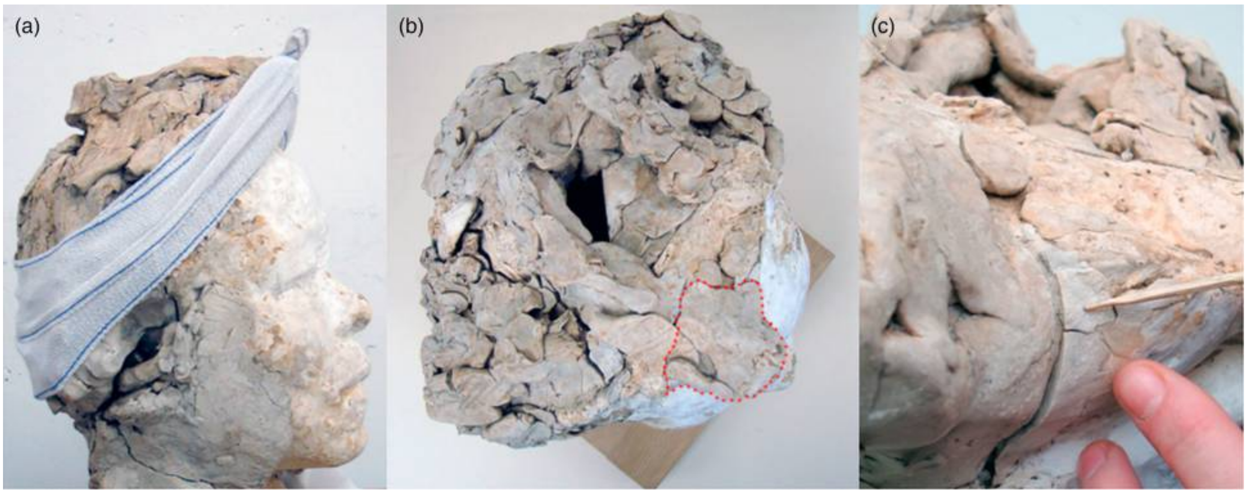


**Figure 11 Conservation treatment of *Hanako* (S.02242). (A) Bonding of the largest detached fragment on the forehead of *Hanako* held in place with a bandage; (B) Top of the head, the large fragment is highlighted with a pointed red line; (C) Consolidation of a flake. Photo credits: H. Bluzat, A. Cascio, and G. Mary.**

distance. Therefore the laser fluence was not calculated precisely for each operation. With the laser spot size settings available from the instrument, a range of theoretical fluences could be evaluated from 0.77 J $cm^{-2}$ (for a 4 mm diameter spot) to 2.5 J $cm^{-2}$ (for a 2 mm diameter spot). No visible surface alterations were noted when observed with a binocular microscope (×20). All traces of modeling details, in particular the fingerprints, were perfectly preserved and the slightly yellow tint of the surface, visible prior to cleaning, remained quite minimal and did not appear to be enhanced by the laser action.

On the slightly hardened and cracked surfaces, satisfactory results were obtained using the laser at low power (Artlight II® Nd:YAG laser 1064 mm, 8 ns pulse at 100 mJ with 10 Hz frequency). All tool traces, including the finest, were retained and sometimes even reappeared if previously hidden by a layer of dust.

In the case of surfaces covered with a thick black crust, the laser at low power was completely inefficient. Somewhat better results were obtained with the stronger laser (Art laser® Nd:YAG laser 1064 mm, 10 ns pulse at 150 mJ with 20 Hz frequency) but presented some risks of surface alteration if distance and power were not carefully controlled. According to the laser settings (used in a range between 2 and 12 mm), we could evaluate the theoretical fluence from 0.13 to 3.75 J.$cm^{-2}$ but this is not the effective fluence applied to the object. The frequency and power settings, as well as the distance to the object, must be very precise. In the zones tested in this way, cleaning was acceptable. It was efficient enough to keep the sculpting traces and fingerprints visible. Even with careful control of distance and power, some slightly yellow coloration could appear with laser cleaning at higher power. Even if this yellowing is negligible and barely visible, we preferred to choose other cleaning methods.

Chemical cleaning using solvents was excluded considering the composition of Rodin's MMM and according to the solvent tests performed. Only water, which presented no danger to the modeling material, was tested in different forms. We added saliva to water, to which it was easily assimilated, for its additional enzymatic properties.

Cleaning methods using a cotton swab, imbibed with water and rolled on the surface, were very quickly eliminated for their inefficiency. Methods using a prolonged application of water poultices were much more efficient. The rehydrated soiling and stains were more easily removed from the somewhat oily surface. A damp cotton swab could then be used to fully eliminate the soiling. In this way, any abrasion of the surface was reduced to a minimum.

The black crusts being particularly thick on *Hanako*, four different cleaning steps were necessary. Preliminary testing showed that it was not advisable to use high-powered laser straight away to eliminate the very thick dirt layer, with the risk of a slightly yellowing on the surface. An initial, partial cleaning was performed at a low-power setting of the laser Artlight (Artlight II® pulse 100 mJ, frequency 10 Hz) on every accessible surface, even though its action remained limited (Fig. 12A). This allowed us to precisely outline the most resistant altered zones.

These specific areas were cleaned by poultices of demineralized water (Fig. 12B). The time necessary to soften the soiling was two hours. The crust was partially or totally removed, depending upon the thickness, thanks to the non-abrasive rolling of the surface with a cotton swab imbibed with water. The thicker crust on the top of the head of *Hanako* was therefore reduced but still remained. The bust of *Clemenceau*, easier to clean, did not require the use of poultices (Fig. 13).

The third step consisted in a second use of the laser at low power (Artlight II® pulse 100 mJ, frequency 10


**Figure 12 Conservation treatment of *Hanako* (S.02242) by laser cleaning. (A) First step: after the initial partial laser cleaning; (B) second step: detail of thick black crusts cleaned by poultices of demineralized water; (C) third step: second use of the laser on the top of the head. Photo credits: H. Bluzat, A. Cascio, and G. Mary.**

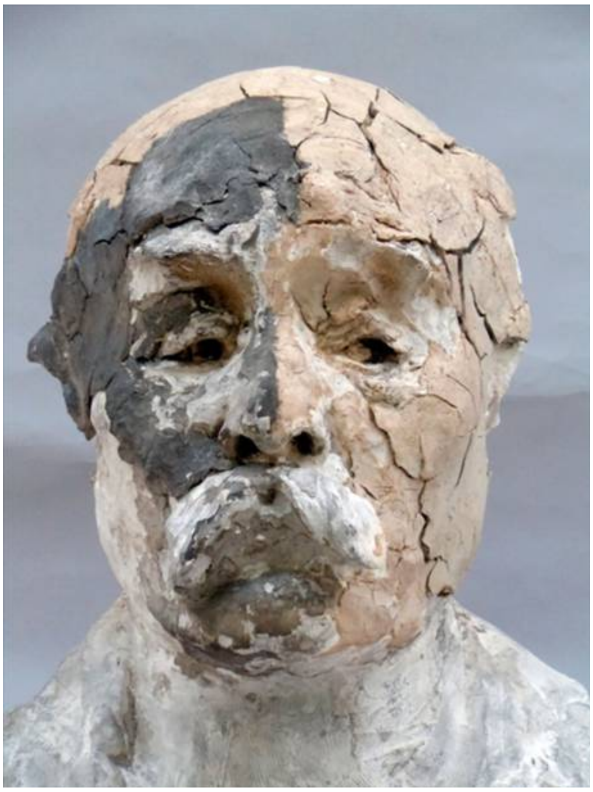

**Figure 13 *Clemenceau* bust (S.01982) during conservation treatment by laser cleaning. The left side shows the state before cleaning and the right after cleaning. Photo credits: H. Bluzat, A. Cascio, and G. Mary.**

Hz) in the finishing stage on the hair of *Hanako* (Fig. 12C). The residual soiling remained dark in comparison with the modeling material which recovered a light color. This contrast guaranteed the efficiency of the laser and, furthermore, avoided any new abrasion of the surface. Nevertheless, the aspect of the modeling material remains yellow in these zones where the especially thick dirt crusts were present. The last step consisted in reapplying poultices of demineralized water on these zones, enabling a maximal reduction of yellowing.

In summary, when applicable, the technique of laser cleaning should be used first because it is by far the least harmful (Fig. 13). But laser cleaning can only be used in cases of light or average soiling. When the black crust layer was too thick, the necessary power needed for cleaning could alter the surface of the modeling material. In this case, other methods were preferable; poultices of water and carboxymethylcellulose applied to an absorbent paper gave good results but only if their application time was extended.

Addition of complexing agents, like EDTA in water, was tested and could help to speed up the water cleaning process but necessitates an additional operation to rinse the complexing agent. Specific tests would be needed to assess the possible interactions between such agents and MMM components (in particular carboxylates, fatty acids), and were not considered in the present study.

### Cleaning the plaster

The plaster was cleaned in a traditional way, by application of a clay gel composed of attapulgite, carboxymethylcellulose, and cellulose powder. This gel was applied in only one 3 mm thick layer, with a soft brush, for one hour. The drying process of the gel was accelerated by ventilation in order to minimize the 'cleansing' action and maintain control of the desired level of cleaning. The areas of modeling material were carefully avoided.

### Inpainting

On the nose of *Hanako* and other minute isolated areas of the face, the outer edge of some fragments of MMM could not be perfectly cleaned. Either these zones were too small and use of the laser could have yellowed the adjacent plaster, or they were too thin to withstand cleaning by dampened cotton swabs. We therefore decided to inpaint the dark areas with watercolors (Winsor & Newton®). When the adhesive fills (Plextol® B500 and micro-glass-beads) maintaining the detached fragments of the right cheek were slightly visible, they were inpainted with the same watercolors.

### Preventive conservation

It is imperative that the sculptures featuring modeling material be stored and exhibited in a stable environment without any noticeable elevation of temperature. Wax and fatty matter are especially sensitive to high and variable temperatures. Humidity should also be regulated as should airborne polluting particles that can aggravate the degradation of these fragile materials. The ideal temperature is situated between 18 and 20°C and should under no circumstances exceed 25°C. The relative humidity should be constant and must be kept at approximately 50%.

Also, the sculptures must be completely protected from dust, because airborne particles have a tendency to adhere to the modeling material. Therefore, the best storage solutions for these sculptures are polyester film covers. The isolation from sulfur can be challenging considering its high presence in plaster and in some MMM composition (group 1); however, any other environmental contribution should be avoided.

## Conclusions

In this work, the composition of different MMMs used by Rodin in 12 of his sculptures was determined. Two main groups were identified. Group 1 is made mainly of zinc oleate, native sulfur, and mineral filler, and group 2 of a mixture of paraffin and fatty matter (as carboxylates), with filler (calcium carbonate). The composition of these two groups 1 and 2 shows similarity with those of the two original 'plastiline' and 'plasticine' recipes described in the historical literature.

The different compositions of group 1 and group 2 resulted in different alterations. The so-called group 2 material was the most frequently used and showed particular alteration features: a rather well spread yellow fatty patina (composed mainly of fatty carboxylates), covered with a gray layer of dust. White protrusions were found to contain high amounts of sulfate crystals, most probably formed by crystallization from environmental sulfur.

Thanks to carefully tested restoration and planned conservation treatment, the head of *Hanako* and the bust of *Clemenceau* can again be presented to the public (Figs. 1C and 2C). They must, however, be manipulated with particular precautions in order to protect their very fragile state despite consolidation. A tailored protocol of conservation–restoration for these plaster sculptures featuring additions in MMM was elaborated following the laboratory analyses and tests in the conservation studio. Nevertheless this protocol cannot be applied systematically, and the nature of the modeling material must be identified before any intervention. These first results could be further complemented by solubility, cleaning, bonding, and consolidation tests on artificially aged samples of MMM. A long-term follow-up of these restored sculptures will provide insight into these issues.

This study of MMMs conserved on Rodin's sculptures was realized with the aim to cover both the scientific analysis of these materials, their degradation process, and the conservation treatment and methodology for two busts of this collection. Our initial findings could be further investigated and confirmed thanks to a thorough examination and detailed analyses of the entire collection of the Musée Rodin. Beyond the case of Rodin's sculptures, it would be interesting to extend this work to various modern and contemporary artists using similar MMMs.

## Acknowledgments

Our thanks go to our sponsor the Hankook Ilbo Cultural Project Centre and most particularly to the director, Sounjou Séo, as well as to the Rodin museum, and especially to the curators François Blanchetière and Hélène Marraud. The authors are grateful to Kimberleight Collins for the translation. The ESRF is thanked for access to beam time. We thank Murielle Salomé, ESRF, for the µXANES analyses of samples from group 1 and Elizabeth Dancer for proofreading of the text.

The editor and reviewers are warmly thanked for their precise and constructive review of our manuscript.

## Appendix

Observations were carried out on cross-sections, by incident light and fluorescent (filter B2A) microscopy. On some of these cross-sections, a chemical spot test was performed during the examination under the microscope to screen for the presence of polysaccharides and in particular starch which is a component often mixed with beeswax. The reagent used was lugol, a solution of elemental iodine ($I_2$) and potassium iodide (KI). A positive reaction of the sample produces a color and for starch this involves the appearance of small black dots.

GC–FID was used on all samples and some additional analyses were performed by GC–MS (samples S.00265, S.01982, S.05703, S.02452, S.02580, and S.02723).

Samples were prepared with a process of derivatization allowing the identification of waxy, oily, and resinous components. The derivatization agent is *N,O*-bis(trimethylsilyl)trifluoroacetamide (BSTFA) containing 1% trimethylchlorosilane. Micro-samples were derivatized with 50 µl of BSTFA/TMCS (99:1) reagent at 80°C for 30 minutes. After a step of evaporation under nitrogen at room temperature, the samples were solubilized in few microliters of dichloromethane prior to injection (1 µl).

The GC–FID instrument is an Agilent 6890 Series fitted with an *on column* injector. The column is a Varian CPSIL 5CB LB/MS capillary column (100% dimethylpolysiloxane phase of 15 m length, 0.32 mm internal diameter, and 0.1 µm film thickness) with a 1 m deactivated pre-column. The temperature was programmed from 50°C (hold time one minute) to 350°C at a rate of 10°C $min^{-1}$ with a final hold time of 10 minutes. Helium was used as carrier gas with a helium ramp flow (1 ml $min^{-2}$ between two different values): 2 ml $min^{-1}$ for 17 minutes; 4 ml $min^{-1}$ for five minutes and 6 ml $min^{-1}$ until the end of the analysis. The *on column* injector was programmed in *track-oven* mode (followed oven temperature + 3°C) and the flame ionization detector temperature was set at 350°C with 35 ml $min^{-1}$ for hydrogen flow and with 300 ml $min^{-1}$ for air flow.

The GC–MS instrument is a single quadrupole GCMS QP2010 Shimadzu system. The capillary column was a Supelco SLB-5ms (30 m length, 0.25 mm internal diameter, and 0.25 µm film thickness, 5% phenyl–95% dimethylpolysiloxane phase). Helium was used as carrier gas with constant linear velocity at 36.3 cm $s^{-1}$. The temperature was programmed from 50 (hold time one minute) to 340°C at a rate of 10°C $min^{-1}$ with a final hold time of 10 minutes. A split–splitless injector was used in splitless mode at 310°C. The MS transfer line was set at 320°C, the ionization source at 200°C. The MS was operated in the electron impact positive ion mode (70 eV) and the scan mode used was from 50 to 950 a.m.u. (atomic mass unity) at 2000 a.m.u. $s^{-1}$.

Bulk FTIR spectra were acquired with a Perkin Elmer Spectrum 2000, using the diamond anvil cell M-A-II from High Pressure Diamond Optics, Inc. (Tucson, AZ). This accessory permits the study of samples without any preparation and their retrieval for future analyses. The spectra were thus collected in transmission mode in 4000–400 $cm^{-1}$ area with a resolution of 4 $cm^{-1}$ and 32 scans. No post-processing was applied to the spectra and identification of compounds was performed by comparison with a spectral database created at the Centre de Recherche et de Restauration des Musées de France (C2RMF) on material of cultural heritage and acquired in the same experimental conditions. Organic and some inorganic components can be identified by this technique.

The XRD experiments were performed with a Rigaku X-ray tube equipped with a copper anode ($\lambda = 1.5418$ Å) and the data were collected with imaging plates as 2D detector Rigaku R-Axis IV. Free software FIT2D was used to transform the two-dimensional images into standard XRD patterns. Then Diffract EVA software program (from Bruker) allowed identification of crystalline phases from XRD patterns thanks to comparison with the PDF database.

SEM–EDX was carried out on most of the cross-sections, after carbon coating, using a Philips XL30CP, a high vacuum electron microscope and an Inca Energy X-ray micro-analysis system. The back-scattered images and analyses were carried out at an accelerating voltage of 20 kV. These elemental analyses offer information about the inorganic components, such as mineral pigments and fillers.

SR-based micro-analyses were carried at the ID21 beamline, at the European Synchrotron Radiation Facility, on fragments from *Two figures embraced on a pillar* (*Deux figures enlacées sur un pilier*, S.05703).

The SR–µFTIR analyses were carried out on the FTIR end-station (Cotte *et al.*, 2008). The microscope is a Continuum, coupled to a Nexus spectrometer, both from Thermo. Samples were prepared as for bulk FTIR (with a diamond anvil cell) but specific attention was paid to orientate properly the sample stratigraphy with respect to the window. The fragment structure is distorted under pressure, but it was still possible to distinguish the different regions. FTIR maps were acquired at low resolution (beam size $25 \times 25$ µ$m^2$) using the Globar source and at high resolution (beam size $8 \times 8$ µ$m^2$) using the synchrotron source. Spectra were acquired as sum of 12 or 32 scans, with a spectral resolution of 8 $cm^{-1}$, in the region 4000–700 $cm^{-1}$. Data were analyzed using the software OMNIC and PyMCA (Sole *et al.*, 2007), using simple regions of interest calculation (intensity over a wavenumber range) and principal component analysis.

SR–μXRF analyses were carried out with the ID21 X-ray microscope. In a few words, the X-ray beam was focused using a Fresnel zone plate to 0.2(V) × 0.9(H) $\mu m^2$. Its energy was selected thanks to a Si111 monochromator. XRF maps were first acquired at 5.1 keV (to detect elements from Na to Ti) then at 3.7 keV (i.e. below the Ca K-edge), revealing the distribution of low Z elements (from Na to K). They were complemented with XANES at the sulfur K-edge (tuning the energy from 2.46 to 2.53 keV), collected in XRF mode. Analyses were carried out under vacuum, both on samples pressed with a diamond anvil cell (following the FTIR analyses) and on samples prepared as embedded cross-sections. Data were analyzed using the PyMCA software (Sole *et al.*, 2007).

### *List of suppliers*

Plastiline® n°50 by J. Herbin (6 avenue de la Trentaine, 77500 Chelles, France)

Plâtre à mouler Molda® 3 Normal by Ceradel (51 rue Presles, 93300 Aubervilliers, France)

Pioloform® BM, BN, and BL18 by Waker chimie S.A. (99 cours Gambetta, 69446 Lyon, France)

Paraloid® B-72 and B-44, Plextol® B500 by Kremer Pigmente (Hauptstr. 41–47, 88317 Aichstetten, Germany)

Tylose® MH300P (methylhydroxyethylcellulose), Primal® E330S, Vinavil® 59 by CTS (26 passage Thiéré, 75011 Paris, France)

Scotchlite® Glass Bubbles K15 by 3M FRANCE (boulevard de l'Oise, 95006 Cergy Pontoise, France)

Aquarelle Winsor & Newton® by Sennelier (3 quai Voltaire, 75007 Paris, France)

Clay gel is composed of:

- Attapulgite Clarsol® by CECA S.A. (Immeuble Iris, 92062 La Défense, France)
- Carboxymethylcellulose, sodium salt by Prolabo – VWR (54 rue Roger Salengro, 94120 Fontenay-sous-Bois, France)
- Cellulose powder Arbocel® type BWW40 by J. Rettenmaïer & Söhne (Holzmühle, 173494 Rosenberg, Germany)

Lasers are distributed by Lambda SpA (Via del Impresa, 136040 Brendola, Italy)

- Artlight II®
- Art laser®

The derivatization agent for GC–MS was supplied by Sigma–Aldrich (Milwaukee, WI).

Dichloromethane, HPLC grade from VWR International, Fontenay-sous-Bois, France.

Sody 33 and its catalytic agent Sody 33 C, by ESCIL, Chassieu, France.

## References


Berrie, B. H., Quillen Lomax, S. & Palmer, M. 2010. Surface and Form: The Effect of Degas' Sculptural Materials. In: S. G. Lindsay, D. S. Barbour, S. Shelley & G. Sturman, eds. *Edgar Degas Sculpture*. Washington: National Gallery of Art, pp. 47–62.

Bertrand, L., Cotte, M., Stampanoni, M., Thoury, M., Marone, F. & Schöder, S. 2012. Development and Trends in Synchrotron Studies of Ancient and Historical Materials. *Physics Reports*, 519(2): 51–96.

Chevreul, M. E. 1823. *Recherches chimiques sur les corps gras d'origine animale*. Paris: F.G. Levrault.

Colinart, S., Drilhon, F., Hours, J. & Scherf, G. 1987. *Sculptures en cire de l'ancienne Egypte à l'art abstrait*. Paris: Réunion des Musées Nationaux.

Cotte, M., Checroun, E., Susini, J., Dumas, P., Tchoreloff, P., Besnard, M. & Walter, P. 2006. Kinetics of Oil Saponification by Lead Salts in Ancient Preparations of Pharmaceutical Lead Plasters and Painting Lead Mediums. *Talanta*, 70(5): 1136–42.

Cotte, M., Checroun, E., Susini, J. & Walter, P. 2007. Micro-analytical Study of Interactions between Oil and Lead Compounds in Paintings. *Applied Physics A: Materials Science & Processing*, 89(4): 841–8.

Cotte, M., Susini, J., Solé, V. A., Taniguchi, Y., Chillida, J., Checroum, E. & Walter, P. 2008. Applications of Synchrotron-based Micro-imaging Techniques to the Chemical Analysis of Ancient Paintings. *Journal of Analytical Atomic Spectrometry*, 23: 820–8.

Delidow, M. & Albertson, C. 2010. Re-thinking the Cleaning of Claes Oldenburg's Floor Cake (Giant Piece of Cake). *AIC Objects Specialty Group Postprints*, 17: 41–64.

Eggert, G. 2006. Plastiline: Another Unsuspected Danger. *Verband der Restauratoren-Beiträge zur Erhaltung von Kunst-und Kulturgut*, 2: 112–6.

Forest, M.-C. 2010. *Gustave Moreau. L'homme aux figures de cire*. Paris: Musée Gustave Moreau, Somogy Edition d'Art.

Giesel, F. 1878. Plastilina. *Berichte der deutschen chemischen Gesellschaft*, 11(1): 310.

Gramtorp, D., Botfeldt, K., Glastrup, J. & Pilkjaer Simonsen, K. 2015. Investigation and Conservation of Anne Marie Carl–Nielsen's Wax Models. *Studies in Conservation*, 60(2): 97–106.

Larochette, Y. 2012. Wolbers' World: A Review of a Textile Wet-Cleaning Workshop Held in Oaxaca, Mexico. *WAAC Newsletter*, 34(1): 24–6.

Lattuati-Derieux, A., Thao, S., Langlois, J. & Regert, M. 2008. First Results on Headspace–solid Phase Microextraction-gas Chromatography/Mass Spectrometry of Volatile Organic Compounds Emitted by Wax Objects in Museums. *Journal of Chromatography A*, 1187(1–2): 239–49.

Mills, J. S. & White, R. 1994. *The Organic Chemistry of Museum Objects*. London: Butterworth- Heinemann.

Moins, P. 2001. *Les Maîtres de la pâte*. Paris: Dreamland.

Raut, J. S., Naik, V. M., Singhal, S. & Juvekar, V. A. 2008. Soap: The Polymorphic Genie of Hierarchically Structured Soft Condensed-Matter Products. *Industrial & Engineering Chemistry Research*, 47(17): 6347–53.

Reau, L. 1930. *Dictionnaire illustré d'art et d'archéologie*. Paris: Larousse.

Regert, M., Colinart, S., Degrand, L. & Decavallas, O. 2001. Chemical Alteration and Use of Beeswax Through Time: Accelerated Ageing Tests and Analysis of Archaeological Samples from Various Environmental Contexts. *Archaeometry*, 43(4): 549–69.

Regert, M., Langlois, J. & Colinart, S. 2005. Characterisation of Wax Works of Art by Gas Chromatographic Procedures. *Journal of Chromatography A*, 1091(1–2): 124–36.

Regert, M., Langlois, J., Laval, E., Le Hô, A. S. & Pagès-Camagna, S. 2006. Elucidation of Molecular and Elementary Composition of Organic and Inorganic Substances Involved in 19th Century Wax Sculptures Using an Integrated Analytical Approach. *Analytica Chimica Acta*, 577(1): 140–52.

Rolfe, M. 1999. *Little Dancer Aged Fourteen: Material Matters*. London: Tate Gallery Publishing Ltd.

Sole, V. A., Papillon, E., Cotte, M., Walter, P. & Susini, J. 2007. A Multiplatform Code for the Analysis of Energy-dispersive X-ray Fluorescence Spectra. *Spectrochimica Acta Part B-Atomic Spectroscopy*, 62(1): 63–8.